DOI 10.1007/s11106-017-9896-2
Powder Metallurgy and Metal Ceramics, Vol. 56, Nos. 5-6, September, 2017 (Russian Original Vol. 56, Nos. 5-6, May-June, 2017)

EFFECT OF VOLUME FRACTION OF REINFORCEMENT AND MILLING TIME ON PHYSICAL AND MECHANICAL PROPERTIES OF Al7075–SiC COMPOSITES FABRICATED BY POWDER METALLURGY METHOD

S. Sattari,[1,4] M. Jahani,[2] and A. Atrian[3]

UDC 669.71;539.4

The volume fraction of reinforcement and milling time are two important factors in fabricating aluminum metal matrix composites via powder metallurgy (P/M) techniques. In the present work, the effects of volume fraction of reinforcement and milling time on the microstructure, relative density, hardness, and compressive strength were studied. The Al7075 and SiC powders were mixed by a planetary ball mill for about 4 and 8 h, and Al7075–x vol.% SiC specimens (x = 4, 6, 8) were fabricated by a uniaxial cold press and sintered at 873 K (600ºC) for 1 h. The crystallite size and morphology of the powder particles were analyzed with X-ray diffraction (XRD) and scanning electron microscopy (SEM), respectively. The results showed that with increasing milling time and volume fraction of the reinforcement phase, the hardness and compressive strength increased. The SEM illustrates that the number of voids increases as SiC content increases, but their size decreases.

Keywords: *Al7075, SiC particles, powder metallurgy, mechanical milling, compressive strength.*

INTRODUCTION

Aluminum alloys, based on Al–Zn–Mg–Cu (7XXX series), are being widely used in some applications such as automotive, marine, military, and aerospace industries due to their low density and appropriate mechanical properties. Among the metal matrix phases, Al7075 is a high performance aluminum alloy with relatively desirable mechanical strength, which has received more attention [1–7]. In recent years, many studies have been done on the aluminum metal matrix composites (AMMCs) as they have high strength-to-weight ratios, low coefficients of thermal expansion, machinability, good damping capacities, and enhanced mechanical properties such as high modulus, high specific stiffness, and fatigue and wear resistance [8, 9].

The different reinforcing materials used in the development of AMMCs can be classified into three broad groups, which are synthetic ceramic particulates, industrial wastes, and agro waste derivatives. Silicon carbide (SiC), alumina(Al_2O_3), boron carbide (B_4C), tungsten carbide (WC), graphite (Gr), carbon nanotubes (CNT), and silica (SiO_2) are some of the synthetic ceramic particulates that have been studied but SiC and Al_2O_3 are mostly utilized

[1]Young Researchers and Elite Club, Najafabad Branch, Islamic Azad University, Najafabad, Iran. [2]Department of Mechanical Engineering, Faculty of Engineering, University of Isfahan, 81746-73441, Isfahan, Iran. [3]Department of Mechanical Engineering, Najafabad Branch, Islamic Azad University, Najafabad, Iran.

[4]To whom correspondence should be addressed; e-mail: Sajjad.Sattari@gmail.com, Sajjad.Sattari@smc.iaun.ac.ir.

Published in Poroshkovaya Metallurgiya, Vol. 56, Nos. 5–6 (515), pp. 60–71, 2017. Original article submitted November 2, 2016.

compared to other synthetic reinforcing particulates [10]. Therefore, SiC is a suitable choice as reinforcement due to its good mechanical properties, thermodynamic stability with aluminum, and also the absence of any detrimental reaction at high temperature [11]. The strength of the particulate (discontinuously) AMMCs is affected by volume fraction, size, shape, and distribution of the particles. However, achieving optimized properties depends on good dispersion of the particles in the matrix [10–12].

The Al7075–SiC composites are fabricated by three different methods: (i) solid-state methods (such as mechanical alloying (MA) and powder metallurgy (P/M)), (ii) molten methods (such as stir casting), and (iii) semi-solid methods [13, 14]. The P/M is one of the methods to fabricate AMMCs that is highly regarded. Lower temperature in fabrication of composites is one of the advantages of this method that reduces the probability of interaction between matrix and reinforcement phases. Uniform and homogeneous reinforcement distribution are other special advantages of this method [12, 13]. Various P/M techniques can be used, mainly quasi-static or dynamic loading. Cold pressing and sintering technology are typical quasistatic fabrication procedures.

Compacting pressure, sintering temperature, and sintering time are effective factors for physical, thermal, and mechanical properties of AMMCs [15–18]. Asgharzadeh [19] studied various compaction pressures ranging 200–1325 MPa and sintering at temperatures between 550 and 650°C for 1 h. His study shows that a temperature of 600°C produces the highest density in all specimens. However, by increasing the compaction pressure, density decreased at the beginning and then increased. Trinh et al. [20] studied CNT–Al composite powders prepared by high-energy ball milling and hot isostatic pressing technique. Their results show that the density and hardness of the CNT–Al composites increased by increasing the sintering temperature up to 620°C and decreased when higher temperature was applied. In order to obtain the best performance of the composite, the sintering temperature was determined to be 620°C. Rahimian et al. [15] studied the effect of sintering temperature and reinforcement content on the properties of Al–Al_2O_3 composite. They concluded that at a temperature of 550°C, the relative density, hardness, and compressive strength were higher than at 500°C. Also, increasing the Al_2O_3 content increased hardness and compressive strength but decreased relative density. They obtained similar results for three different temperatures of 500, 550, and 600°C, but at a temperature of 600°C, the physical and mechanical properties were reported to be higher [16].

In this study, the Al7075 specimens reinforced with SiC particles (4, 6, 8 vol.%) were fabricated by mechanical milling, cold pressing, and sintering at 873 K (600°C) for 1 h. The effects of volume fraction of reinforcement and milling time on the relative density, hardness, and compressive behavior of specimens were studied.

MATERIALS AND EXPERIMENTAL PROCEDURE

The Al7075 powder as the matrix (gas atomized, 150 μm, irregular morphology) and SiC as the reinforcing particles (average 20 μm) were milled in a planetary ball mill. Figure 1 shows the morphology of as-received material.

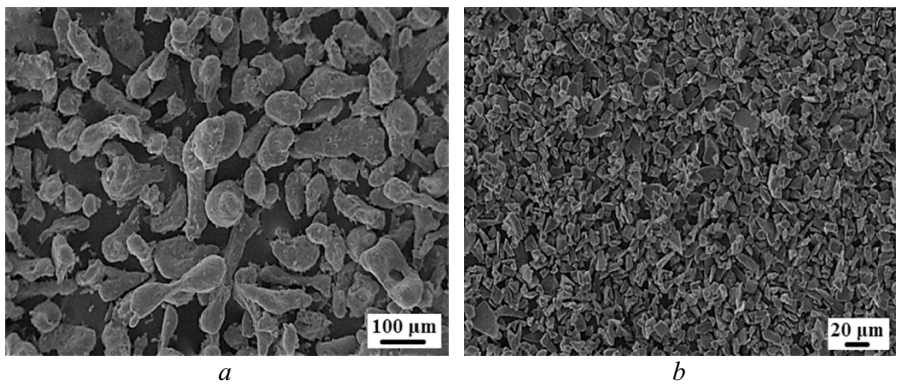

a *b*

Fig. 1. SEM micrographs of (*a*) Al7075 and (*b*) SiC particles

Chemical composition of Al7075 is shown below:

Chemical Composition of Al7075 (in wt.%)

Zn	Mg	Cu	Cr	Fe	Mn	Si	Ti	V	Al
5.6	2.5	1.42	0.19	0.15	0.06	0.09	0.08	0.006	Remaining

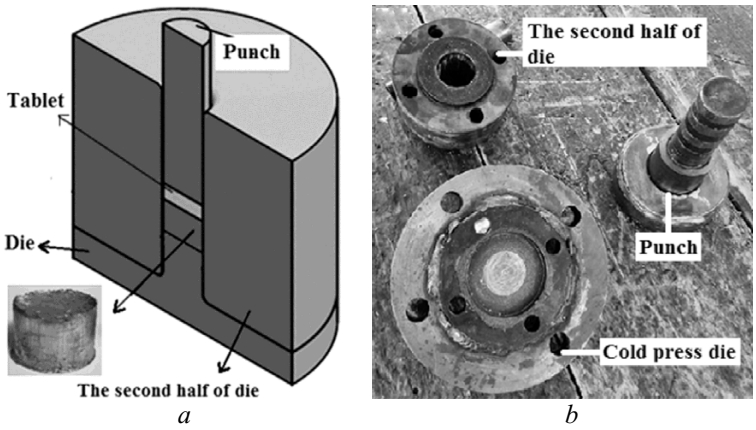

a *b*

Fig. 2. Schematic of cold compacted (*a*) and punch and dies (*b*) used in this work

TABLE 1. Mechanical Milling Conditions

Factors	Value
Ball-to-powder mass ratio (BPR)	10
Rotational speed (rpm)	600
Time (h)	4, 6, 8
Ball material	Stainless steel
Process control agent (PCA)	Stearic acid, 1 wt.%
Atmosphere	Argon, 99.99% purity

Table 1 indicates effective factors in mechanical milling process. In order to avoid overheating of the powder mixture, milling was stopped for 15 min after each hour. After milling, the powders were degassed at 673 K (400°C) for 2 h to remove moisture, adsorbed hydrogen, and oxygen. The milled powder mixture was wrapped using an aluminum foil and then cold compacted under a uniaxial pressure of 430 MPa for 10 min. The compacted samples were sintered at 873 K (600°C) for 1 h in an argon atmosphere using a tube furnace.

Figure 2 shows the punch and dies that were used in this study. The compaction was performed in a cylindrical steel die with inner diameter 35 mm, outside diameter 120 mm, and height 80 mm. In Fig. 2*a*, a tablet with a thickness of 5 mm is used. The tablet assists the compacted specimens to be pulled out from the die more easily.

In order to study the structural change during mechanical milling process and evaluate the crystallite size, the XRD patterns of powders were recorded using a PHILIPS X' PERT PW3040 diffractometer (40 kV/30 mA) with Cu-K_α radiation ($\lambda = 0.154059$). Compression test was done according to ASTM E9 and at room temperature at a speed of 3 mm/min and an aspect ratio (length-to-diameter) of 1.5. The hardness of samples was measured by the Brinell hardness test with a ball diameter of 2.5 mm and 30 kg force (according to ASTM E10).

RESULTS AND DISCUSSION

Characterization. Figure 3 shows XRD patterns of composite powder with different amounts of SiC and after 4 and 8 h milling; it also reveals that the milled powder includes only Al and SiC and no new phase are produced as a result of milling and there are not any metal combinations. In fact, increasing the temperature during

the milling process was not sufficient for SiC decomposition and formation of intermetallic compounds of carbon and silicon. In addition, because of controlling the milling atmosphere, any unwanted oxide compounds were not found.

The crystallite size and the lattice strain of the milled aluminum powders are estimated by XRD peak broadening using the Williamson–Hall method (Eq. (1)):

$$B\cos\theta = (0.9\lambda/D) + 2\varepsilon\sin\theta, \quad (1)$$

where B is full width at half maximum intensity (FWHM); θ is the Bragg diffraction angle; λ is the wavelength of the radiation used; D is the average crystallite size; and ε is the average lattice strain which can be estimated from the linear slope of $B\cos\theta$ versus $\sin\theta$. The average crystallite size is the value of the slope at $\sin\theta = 0$ [1, 17]. Figure 4 shows the changes of matrix grain size and lattice strain of the Al7075–SiC composite powder (calculated by the Williamson–Hall method) depending on the SiC content and milling time. As expected, severe plastic deformation (SPD) of powder particles during milling process reduced the size of aluminum-based crystals to nanometers. Therefore, the size of matrix grains decreased to less than 100 nm.

As shown in Fig. 4, the crystallite size decreases by increasing the milling time, down to 39 and 37 nm for 6 and 8 vol.% SiC, respectively. This event has been reported by several researchers as well [1, 6, 13, 21, 22]. Also, the crystallite size decreases by increasing SiC content, which has been similarly reported by other researchers [6, 13]. On the other hand, the effect of the milling time on the lattice strain of the examined powder particles is presented in Fig. 4.

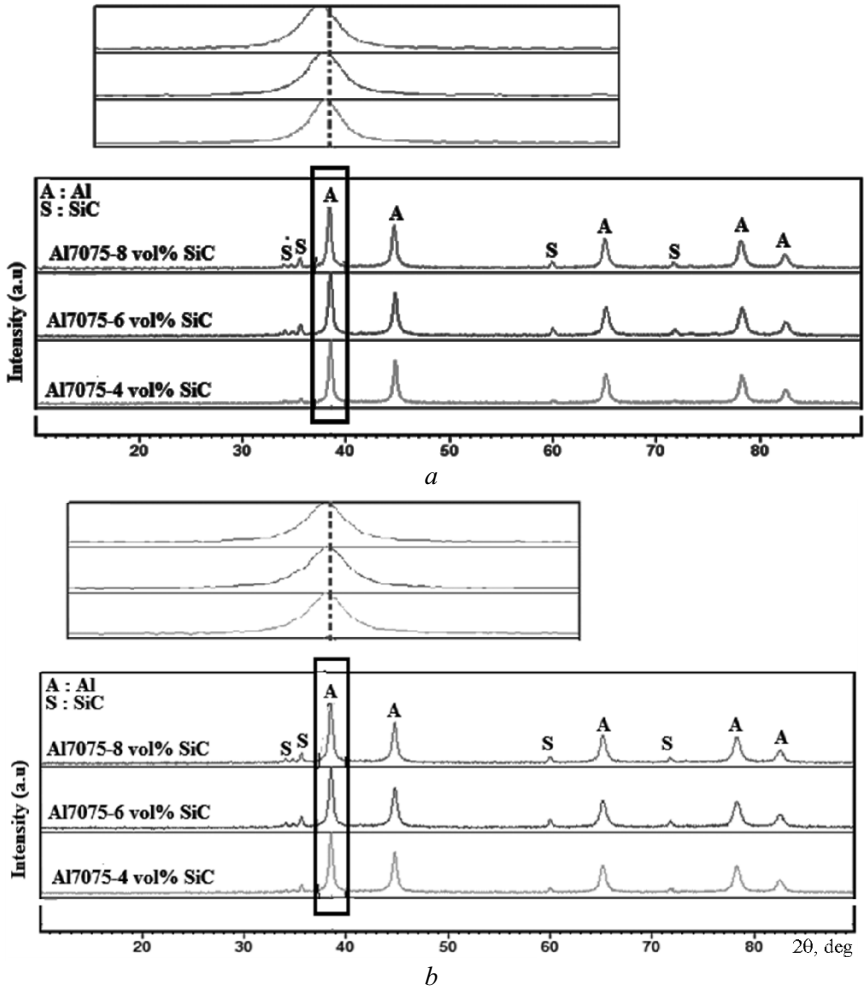

Fig. 3. XRD patterns of Al7075–SiC powders after (*a*) 4 h and (*b*) 8 h milling

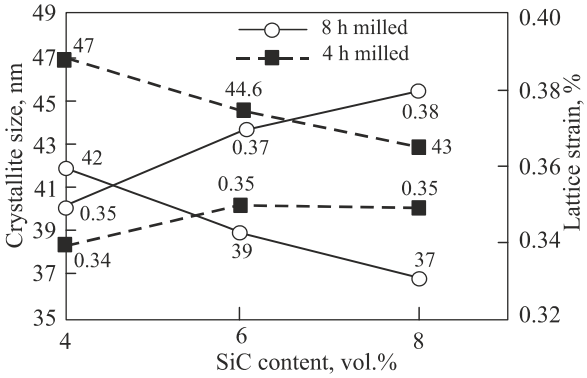

Fig. 4. Crystallite size and lattice strain of Al7075–SiC composite powders after 4 and 8 h milling

It has been indicated that the lattice strain of the powder particles shows an increasing tendency. It can be seen that as the milling time increases, the Al peaks are gradually broadened and their intensities decrease, which is believed to be due to an increase in the lattice strain and a decrease in the crystallite size.

The stress generated by plastic deformation causes the formation of subgrain boundaries and, therefore, grain refinement will be observed with increasing of the lattice distortion. Azimi et al. [1] reported that by increasing

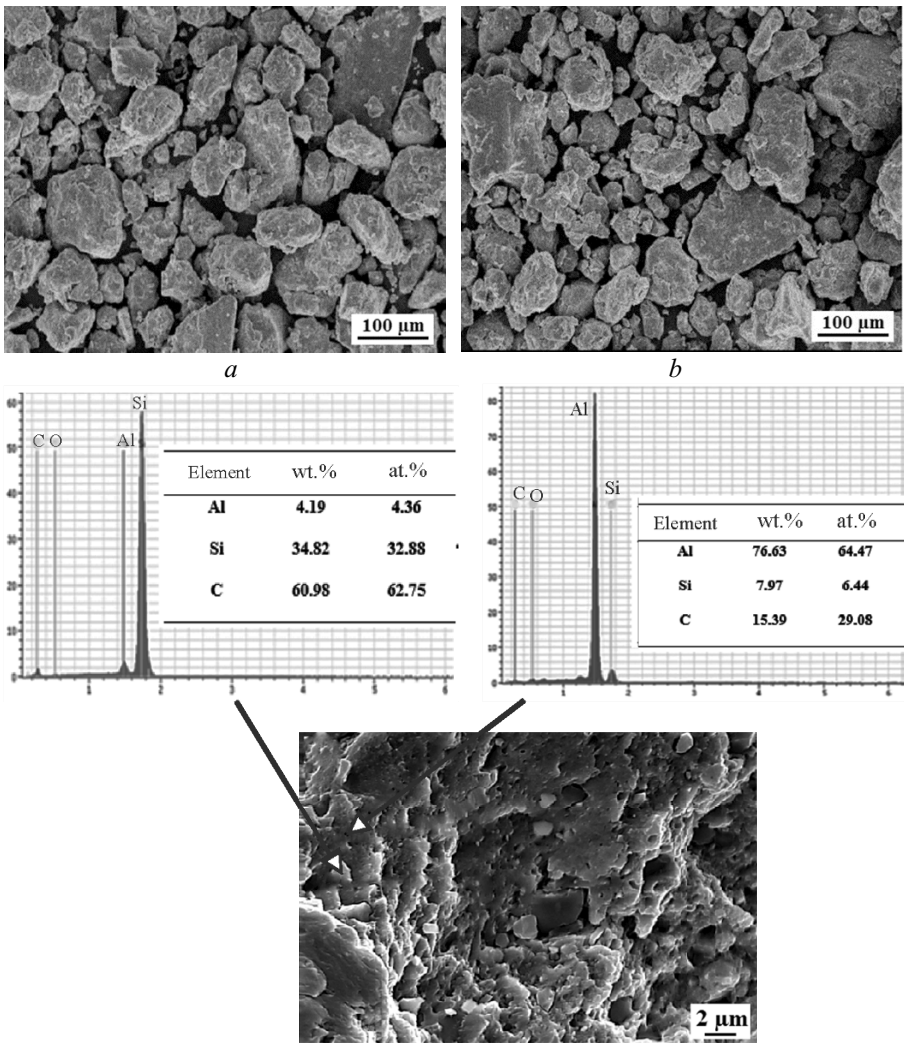

Fig. 5. Al7075–6 vol.% SiC after 4 h milling (*a*); Al7075–6 vol.% SiC after 8 h milling (*b*, *c*)

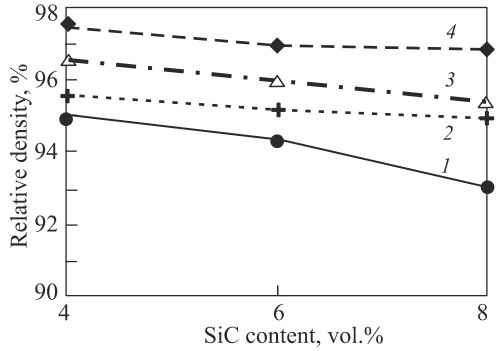

Fig. 6. Variations of relative densities versus SiC content: *1*, *3*) 4 h before and after sintering, respectively; *2*, *4*) 8 h before and after sintering, respectively

the milling time from 10 to 50 h, the crystallite size of Al7075–TiC decreased and lattice strain increased. Figure 5 shows the SEM of micrographs for the Al7075–SiC powder mixtures, after 4 and 8 h milling.

In general, there are three main mechanisms for particle morphology changes in the mechanical milling process including: (i) plastic deformation mechanism, (ii) cold welding mechanism, and (iii) fracture mechanism. In the first step, the powder particles slip over each other by the modes of fracture and plastic deformation mechanism. In the second step, powder particles deform as a little elastic and plastic deformation and cold welding occur between them. In the third step, the powder particles were hard worked and failed. The Al–SiC powder under mechanical milling process is ductile–brittle, which is the main reason of particle agglomerations in the presence of aluminum as ductile particles because aluminum is a metal with high ductility that at the beginning, due to lack of balance between the cold welding ratio and fracture of powder particles, has a tendency to agglomeration. With increasing milling time, at first a relative balance is established between the cold welding ratio and fracture and then, with its further increasing, tendency to fracture will be higher than cold welding [23–25].

As shown in Fig. 5, the powder particle size decreases as the milling time increases, which is probably due to the two opposing factors of cold welding and fracturing of powder particles.

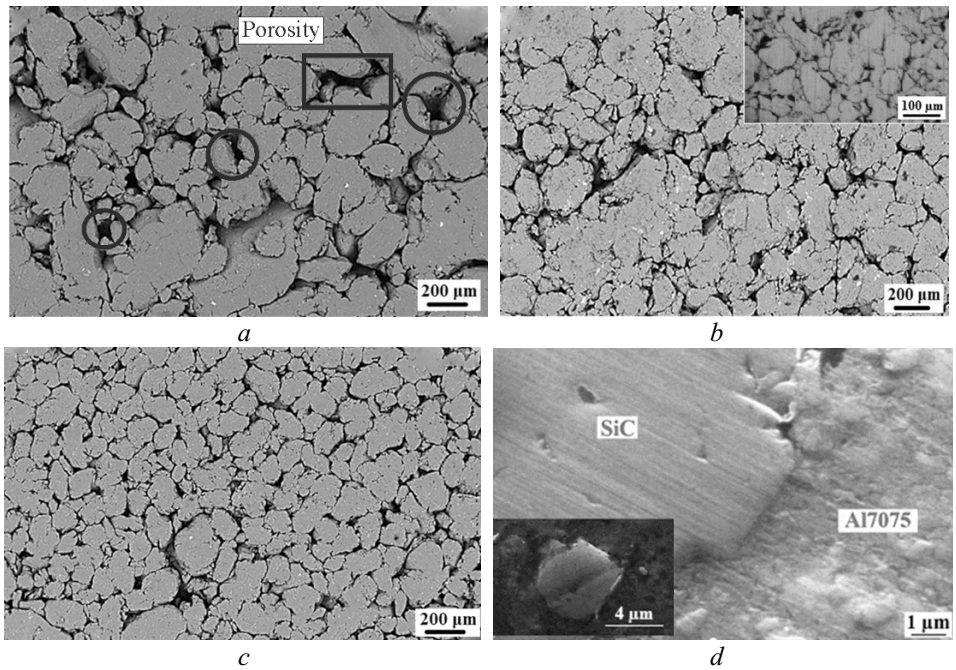

Fig. 7. SEM micrographs of Al7075–4 vol.% SiC (*a*), Al7075–6 vol.% SiC (*b*), Al7075–8 vol.% SiC (*c*) after 8 h milling, and interface between SiC and Al7075 (*d*)

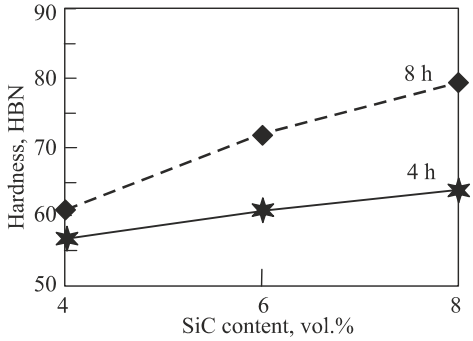

Fig. 8. Effects of milling time and SiC content on hardness of Al7075–SiC

Density. Microstructure changes during the milling process can affect the pressability and porosity of samples. To examine this property, the density of various samples was measured by the Archimedes method that is presented in Fig. 6. The results show that the relative density increases after sintering. It is obvious that the temperature is proportional to the growth of neck area between particles. The higher the temperature, the easier and greater the diffusion that increases the density of composites. The diffusion coefficient and sintering temperature are related by Eq. (2) [15, 16]:

$$D = D_0 \exp\left(-\frac{Q}{RT}\right), \tag{2}$$

where D is the diffusion coefficient; D_0 is constant; Q is the activation energy; R is Boltzman's constant; and T is temperature. Sintering temperature is the controlling factor in sintering mechanism. The proper temperature of sintering provides conditions for diffusion of atoms to reduce the amount of porosity and thus increase density. Generally, compaction and sintering of composite materials are different from those of single-phase materials. The presence of hard and nondeformable particles in a ductile matrix reduces the pressability of the material. The reduction in pressability increases for higher volume fraction of reinforcement phase [17]. Figure 7 demonstrates SEM micrographs of Al7075–SiC for different contents of SiC particles. As can be seen, the number of the voids increases as SiC content increases, but their size decreases. Figure 7*d* in higher magnification shows appropriate bonding between the SiC particles and aluminum matrix. Due to matrix ductility and high wettability, the matrix covers the whole SiC particles. These cause applied forces to the composite to be tolerated by both phases. Usually, the reinforcement that possesses higher strength takes on the main load and the matrix transforms load to the reinforcement. This bonding in the zone between the matrix and reinforcement phase (interface or interphase) improves mechanical properties.

Hardness. Hardness represents the resistance of material to plastic deformation which is caused by penetration of the indenter. Figure 8 shows the effects of milling time and volume fraction of reinforcement on hardness of the Al7075–SiC composite.

As can be seen, the hardness value of the specimens increases with increasing the SiC content and milling time. The rule of mixtures and Hall–Petch effect could be pointed out as reasons of increasing hardness.

- Rule of mixtures:

$$H_c = H_m f_m + H_r F_r, \tag{3}$$

where H_c, H_m, and H_r are the hardness of composite, matrix, and reinforcement; f_m and f_r are volume fraction of matrix and reinforcement, respectively. It was observed from Fig. 8 that by increasing the volume fraction of SiC particles from 4 to 8%, hardness increased from 57 to 64 HBN in 4 h milling and from 61 to 79 HBN in 8 h milling.

- Hall–Petch effect:

$$H + H_0 + KD^{-0.5}, \tag{4}$$

where H and H_0 are the hardness of composite and annealed coarse-grained sample; K and D are a constant number and grain size, respectively. It is expected that by refining the grain size of matrix phase, the hardness of samples

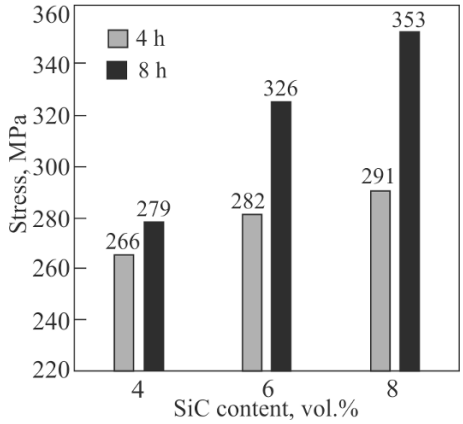

Fig. 9. Effects of milling time and SiC content on ultimate compressive strength of Al7075–SiC

rises. Therefore, enhancement of hardness due to the structure grain refinement after milling is not unexpected. Similar observations have been reported by El-Kady [12], Abdollahi [13], and Ghasemi Yazdabadi [22].

Compressive Strength. Figure 9 shows the compressive strength value of two kinds of composites as a function of volume fraction of SiC and the milling time. As shown in this figure, the ultimate compressive strength increases with increasing the SiC content and milling time.

To study the strengthening effects of SiC particles on the compressive properties of the composites, two approaches have been used which have been reported by researchers in recent years.

(i) Continuum mechanics [26–30]:

- The load transferring effect from ductile matrix to reinforcement particles, which requires good bonding between the matrix and SiC particles.

(ii) Micromechanics strengthening [26–30]:

- Hall–Petch effect ($\sigma = \sigma_0 + kd^{-0.5}$) due to grain refinement that could provide more area to resist the dislocation movements.
- Orowan strengthening mechanism ($T = Gb/\lambda$) due to fabrication of Al–SiC composite samples by mechanical milling, distance between the particles reduces and required stress to pass dislocations among reinforcement particles becomes higher and thus their strength will be greater. According to the Orowan strengthening mechanism, dislocation loops provide more resistance to the movement of dislocations.
- Strengthening arises from increase in dislocation density of the matrix due to the mismatch of coefficients of thermal expansion (CTEs) between SiC and the Al7075 matrix (1 : 8) ($\alpha_{SiC} = 2.77 \cdot 10^{-6}$/K, $\alpha_{Al7075} = 23.2 \times \times 10^{-6}$/K) and between processing and test temperatures ($\Delta T = 848$ K (575°C)). These dislocations make the plastic deformation more difficult.

CONCLUSIONS

The Al–SiC composite was successfully fabricated by employing high-energy ball milling with cold pressing and sintering technology at 873 K (600°C) for 1 h.

During the mechanical milling, the crystallite size decreases with increasing the milling time. After 8 h milling, the crystallite size of the composite was 37 nm for 8 vol.% SiC.

The physical and mechanical properties of the specimens were studied using density, hardness, and compressive strength tests. The relative density increased after sintering. For example, for the 8 vol.% SiC specimen, the relative density increased from 95 to 96.9 after 8 h milling.

Also, the SEM illustrated that with increasing SiC content, the number of the voids increased, but their size decreased. The compressive strength of the composites increased with increasing the SiC content and milling time. The same tendency as the strength was observed for the hardness value. The hardness of the composite after 8 h milling was 79 HBN for 8 vol.% SiC.

REFERENCES

1. A. Azimi, A. Shokuhfar, and O. Nejadseyfi, "Mechanically alloyed Al7075–TiC nanocomposite: Powder processing, consolidation and mechanical strength," *Mater. Des*., **66**, Part A, 137–141 (2015).
2. H. R. Hafizpour and A. Simchi, "Investigation on compressibility of Al–SiC composite powders," *Powder Metall*., Vol. **51**, No. 3, 217–223 (2008).
3. M. A. Jabbari Taleghani, E. M. Ruiz Navas, and J. M. Torralba, "Microstructural and mechanical characterization of 7075 aluminum alloy consolidated from a premixed powder by cold compaction and hot extrusion," *Mater. Des*., **55**, 674–682 (2014).
4. Y. Jia, F. Cao, Z. Ning, et al., "Influence of second phases on mechanical properties of spray-deposited Al–Zn–Mg–Cu alloy," *Mater. Des*., **40**, 536–540 (2012).
5. S. Kamrani, A. Simchi, R. Riedel, and S. M. Seyed Reihani, "Effect of reinforcement volume fraction on mechanical alloying of Al–SiC nanocomposite powders," *Powder Metall*., **50**, No. 3, 276–282 (2007).
6. M. A. Mobarhan Bonab and A. Simchi, "Effect of silicon carbide nanoparticles on hot deformation of ultrafine-grained aluminum nanocomposites prepared by hot powder extrusion process," *Powder Metall*., **59**, No. 4, 262–270 (2016).
7. Z. G. Wang, C. P. Li, H. Y. Wang, et al., "Effect of nano-SiC content on mechanical properties of SiC/2014Al composites fabricated by powder metallurgy combined with hot extrusion," *Powder Metall*., **59**, No. 4, 236–241 (2016).
8. G. B. Schaffer and S. H. Huo, "On development of sintered 7xxx series aluminum alloys," *Powder Metall*., Vol. **42**, No. 3, 219–226 (1999).
9. A. A. El-Daly, M. Abdelhameed, M. Hashish, and W. M. Daoush, "Fabrication of silicon carbide reinforced aluminum matrix nanocomposites and characterization of its mechanical properties using non-destructive technique," *Mater. Sci. Eng. A*., **559**, 384–393 (2013).
10. M. O. Bodunrin, K. K. Alaneme, and L. H. Chown, "Aluminum matrix hybrid composites: a review of reinforcement philosophies; mechanical, corrosion and tribological characteristics," *J. Mater. Res. Technol*., No. 4, 434–445 (2015).
11. R. Senthilkumar, N. Arunkumar, and M. Manzoor Hussian, "A comparative study on low cycle fatigue behavior of nano and micro Al_2O_3 reinforced AA2014 particulate hybrid composites," *Results Phys*., **5**, 273–280 (2015).
12. O. El-Kady and A. Fathy, "Effect of SiC particle size on the physical and mechanical properties of extruded Al matrix nanocomposites," *Mater. Des*., **54**, 348–353 (2014).
13. A. Abdollahi, A. Alizadeh, and H. R. Baharvandi, "Dry sliding tribological behavior and mechanical properties of Al2024–5 wt.% B_4C nanocomposite produced by mechanical milling and hot extrusion," *Mater. Des*., **55**, 471–481 (2014).
14. M. Khademian, A. Alizadeh, and A. Abdollahi, "Fabrication and characterization of hot rolled and hot extruded boron carbide (B_4C) reinforced A356 aluminum alloy matrix composites produced by stir casting method," *Trans. Indian Inst. Met*., 1–12 (2016).
15. M. Rahimian, N. Ehsani, N. Parvin, and H. R. Baharvandi, "The effect of sintering temperature and the amount of reinforcement on the properties of Al–Al_2O_3 composite," *Mater. Des*., **30**, No. 8, 3333–3337 (2009).
16. M. Rahimian, N. Ehsani, N. Parvin, and H. R. Baharvandi, "The effect of particle size, sintering temperature and sintering time on the properties of Al–Al_2O_3 composites, made by powder metallurgy," *J. Mater. Process. Technol*., **209**, No. 14, 5387–5393 (2009).
17. S. S. Razavi-Tousi, R. Yazdani-Rad, and S. A. Manafi, "Effect of volume fraction and particle size of alumina reinforcement on compaction and densification behavior of Al–Al_2O_3 nanocomposites," *Mater. Sci. Eng. A*., **528**, No. 3, 1105–1110 (2011).

18. Z. Wei, P. Ma, H. Wang, et al. “The thermal expansion behaviour of SiCp/Al–20Si composites solidified under high pressures,” *Mater. Des.*, **65**, 387–394 (2015).
19. H. Asgharzadeh, “Sintering behavior of nanocrystalline Al6063 powders prepared by high-energy mechanical milling,” *Trans. Indian Inst. Met*., **69**, No. 7, 1359–1368 (2016).
20. P. Van Trinh, N. Van Luan, P. N. Minh, and D. D. Phuong, “Effect of sintering temperature on properties of CNT/Al composite prepared by capsule-free hot isostatic pressing technique, **69**, No. 7, 1–9 (2016).
21. A. Alizadeh, and E. Taheri-Nassaj, “Mechanical properties and wear behavior of Al–2 wt.% Cu alloy composites reinforced by B_4C nanoparticles and fabricated by mechanical milling and hot extrusion,” *Mater. Charact*., **67**, 119–128 (2012).
22. H. Ghasemi Yazdabadi, A. Ekrami, H. S. Kim, and A. Simchi, “An investigation on the fatigue fracture of P/M Al–SiC nanocomposites,” *Metall. Mater. Trans. A*., **44**, No. 6, 2662–2671 (2013).
23. C. Suryanarayana, “Mechanical alloying and milling,” *Prog. Mater. Sci.,* **46**, Nos. 1–2, 1–184 (2001).
24. C. Suryanarayana, E. Ivanov, and V. V. Boldyrev, “The science and technology of mechanical alloying,” *Mater. Sci. Eng. A*., **304–306**, 151–158 (2001).
25. D. L. Zhang, “Processing of advanced materials using high-energy mechanical milling,” *Prog. Mater. Sci*., **79**, Nos. 3–4, 537–560 (2004).
26. H. Simchi and A. Simchi, “Tensile and fatigue fracture of nanometric alumina reinforced copper with bimodal grain size distribution,” *Mater. Sci. Eng. A*., **507**, Nos. 1–2, 200–206 (2009).
27. F. Chen, Z. Chen, F. Mao, et al., “TiB_2 reinforced aluminum based in situ composites fabricated by stir casting,” *Mater. Sci. Eng. A*., **625**, 357–368 (2015).
28. T. Wang, Z. Chen, Y. Zheng, et al., “Development of TiB_2 reinforced aluminum foundry alloy based in situ composites. Part II: Enhancing the practical aluminum foundry alloys using the improved Al–5 wt.% TiB_2 master composite upon dilution,” *Mater. Sci. Eng. A*., **605**, 22–32 (2014).
29. S. Sattari and A. Atrian, “Effects of the deep rolling process on the surface roughness and properties of an Al−3 vol.% SiC nanoparticle nanocomposite fabricated by mechanical milling and hot extrusion,” *Int. J. Minerals, Metallurgy, Materials*,” **24**, Issue 7, 814–825 (2017).
30. S. Sattari and M. Jahani, “An investigation of parameters involved and defects in the fabrication of Al–SiC nanocomposite using hot extrusion technique,” *Transac. Indian Inst. Metals*., DOI: 10.1007/s12666-017-1097-7, 1–10 (2017).